Available online at www.sciencedirect.com

ScienceDirect

Catalysis Today 131 (2008) 427–430

CATALYSIS TODAY

www.elsevier.com/locate/cattod

Methanol oxidation on LaCo mixed oxide supported onto MCM-41 molecular sieve

E.V. Makshina [a], N.S. Nesterenko [a], S. Siffert [b,*], E.A. Zhilinskaya [b],
A. Aboukais [b], B.V. Romanovsky [a]

[a] *Department of Chemistry, M.V. Lomonosov Moscow State University, Leninskie Gory 1, Building 3, 119992 Moscow, Russia*
[b] *Laboratory of Catalysis and Environment, E.A. 2598, University of Littoral – Côte d'Opale, 145 Avenue Schumann, 59140 Dunkerque, France*

Abstract

Lanthanum cobaltate $LaCoO_x$ supported onto MCM-41 mesoporous molecular sieve was prepared by *in-situ* oxidative decomposition of mixed LaCo citrate complexes inside the mesopores of this support. The prepared materials were characterized by EDX, EPR and UV-Vis DRS techniques as well as by N_2-BET measurements. The nanosized $LaCoO_x$ particles within the mesopores of MCM-41 matrix contains cobalt atoms in lower than Co(III) average oxidation state. Also, the supported cobaltate does not form short-range order species of $LaCoO_3$ but presents as the highly disordered, oxygen deficient Co oxide nanophase. Catalytic activity in MeOH oxidation was tested using both conventional fixed-bed flow system and ‘‘operando'' mode of DRIFT technique. The very high activity of MCM-41-supported cobaltate is not only due to highly dispersed $LaCoO_3$ phase but also because of rather low oxidation state of Co.

Keywords: Perovskite; Nanostructured $LaCoO_3$; MCM-41; Methanol oxidation

1. Introduction

Mixed oxides with perovskite-like structure have attracted extensive attention in recent years because of the high efficiency in both oxidation catalysis and membrane technology due to surprisingly high mobility of structural oxygen. In some cases, the activity of perovskite materials was shown to be almost the same and even higher than that of conventional Pt-containing catalysts for oxidation of VOC. However, the bulk perovskites prepared via conventional synthetic procedures exhibits rather small surface areas of a few tens of m^2/g [1] which restricts strongly the applications of these materials as catalysts. One of the most perspective ways to increase the surface area of perovskites is supporting them onto porous solid matrices. While there have been a large number of studies on the supported perovskites using traditional oxide supports such as Al_2O_3, SiO_2, ZrO_2 etc., similar works on molecular sieve supports are rather scarce. In this respect, mesoporous molecular sieves of M41S type with well controlled pore size seem to be of special interest as promising porous solids to support the perovskite oxides. Moreover, MCM-41 presents also a regular porous structure like zeolite but with larger pore diameter (~3 nm) than zeolite (<1 nm) allowing the synthesis of oxide nanoclusters in the nanoreactors of the mesoporous molecular sieves. Thus our recent characterization works by XPS and XAFS [2] of the $LaCoO_x$/MCM-41 samples used in this paper proved the formation of highly disordered nanosized oxide particles located inside the mesopores of the molecular sieve.

In this work, we report new characterizations of the nanostructured La cobaltate loaded on the mesoporous MCM-41 molecular sieve and mesoporous SiO_2 by EDX, EPR, UV-Vis DRS and also the study of its activity in MeOH oxidation by conventional and operando mode of DRIFT technique.

2. Experimental

Supported cobaltate was prepared by impregnation of air-dry molecular sieve MCM-41 (surface area 1150 m^2/g, pore diameter 3.1 nm) and silicagel (380 m^2/g, 6.2 nm) with LaCo citrate aqueous solution [3]. After drying at 60–65 °C, the

---

* Corresponding author. Tel.: +33 3 28 65 82 56; fax: +33 3 28 65 82 39.
E-mail address: siffert@univ-littoral.fr (S. Siffert).

0920-5861/$ – see front matter © 2007 Elsevier B.V. All rights reserved.
doi:10.1016/j.cattod.2007.10.088

samples were calcined at 600 °C for 8 h in dry airflow. These samples with ~10 wt.% of La cobaltate is denoted as $LaCoO_x$/MCM-41 and $LaCoO_x/SiO_2$. Also, bulk $LaCoO_3$ perovskite was synthesized using the standard citrate method [4], bulk cobalt oxide Co_3O_4 was prepared by evaporation of Co citrate solution until dry followed by calcination at 600 °C for 8 h.

Atomic absorption spectroscopy was used to analyze the chemical composition of samples. Also, the metal composition of the samples was determined by EDX analysis using a scanning electron microscope JEOL JMS-840A equipped with a PGT IMIX system. N_2-BET surface area measurements were carried out at 77 K using a Micromeritics ASAP 2000N instrument. XRD patterns of the materials were recorded on a Bruker D8 Advance diffractometer in the $2\theta = 2$–8° range using Cu Kα radiation. EPR spectra for air-dried samples were measured at 77 and 293 K on a Bruker EMX spectrometer (9.3 GHz) with 100 kHz high-frequency modulation. Diffuse reflectance UV–vis spectra were collected on a Varian CARY 500 UV-vis-IR spectrometer.

The catalytic activity in methanol oxidation was also evaluated using two different methods. (i) A fixed-bed quartz reactor operating at 100–225 °C, 0.101 MPa and WHSV = 0.7 h^{-1} was used, the main reaction products (ca. 99%) were carbon dioxide and formaldehyde. (ii) An ‘‘operando’’ mode of diffuse reflectance technique was employed using FTIR Bruker Equinox 55 equipped with the ‘‘Praying Mantis’’ and the ‘‘high reaction chamber’’ from Harrick Scientific Corp.

3. Results and discussion

The chemical composition and textural properties of the prepared samples is given in Table 1. Incorporation of $LaCoO_x$ oxide into the pores of both MCM-41 and SiO_2 supports results in negligible decrease of mesopores volume and specific areas. It should be noted that the shape of the adsorption isotherms did not change noticeably after loading supports with metal oxide as well as the pore distribution [2]. This means that the supports are not destroyed during the synthetic procedures.

At large angles, the XRD pattern for bulk $LaCoO_3$ showed the peaks characteristic of pure perovskite phase (JCPDS file No. 25-1060). In contrast, supported $LaCoO_x$/MCM-41 is X-ray amorphous. This suggests though indirectly that the $LaCoO_x$ particles formed within the mesoporous MCM-41 are not exceeding the 3-nm diameter of the host pores.

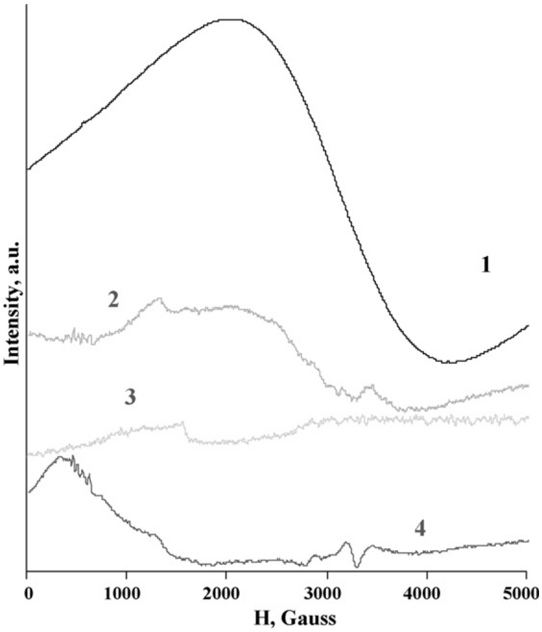

Fig. 1. EPR spectra at $T = 293$ K of bulk and supported samples: (1) Co_3O_4, (2) $LaCoO_3$, (3) $LaCoO_x/SiO_2$ and (4) $LaCoO_x$/MCM-41.

Results in our previous work [2] presenting the small-angle XRD for MCM-41 mesoporous material confirmed the hexagonal structure of this material by a very intense diffraction peak at $2\theta = 2.3°$ and two weak peaks at $2\theta = 4.1°$ and 4.7°. After loading the LaCo oxide species, the first signal was found to strongly decrease and the weaker signals disappeared at all. Such attenuation of the XRD signals of ordered silicate matrices may be also expected upon statistical distribution of heavy matter over the pore system because of the modified scattering contrast between pore walls and pores [5].

EPR spectrum of supported cobaltate $LaCoO_x$/MCM-41 at $T = 293$ K (Fig. 1) represents of a broad high asymmetric line (average g-factor $\bar{g} \sim 5.4$) that is shifted noticeably toward the low-field region in comparison with the spectrum of bulk perovskite. On decreasing the registration temperature from 295 to 77 K, the signal width and intensity of supported cobaltate increase and a low-field maximum of signal shifts to the low fields. The same behaviour of EPR spectra has been observed for isolated Co(II) ions in ion-exchanged A and X zeolites [6]. According to [6–8] the signal with $\bar{g} \sim 5.4$ can be attributed to the isolated octahedrally coordinated Co(II) ions with some tetragonal or trigonal distortions. As the EPR signal with $\bar{g} \sim 2.3$ corresponding to Co_3O_4 was not observed for

Table 1
Textural properties of the samples

Sample	Chemical composition (wt.%)		Atomic La/Co	S_g (m^2/g)	V_{meso} (cm^3/g)	Pore diameter (Å)
	La	Co				
$LaCoO_3$	50.1	22.0	1:1	10.4	–	–
MCM-41	–	–	–	1150	0.73	30
SiO_2	–	–	–	380	0.55	55
$LaCoO_x$/MCM-41	5.53	2.46	1:1	1007	0.53	29
$LaCoO_x/SiO_2$	5.46	2.38	1:1	335	0.52	55

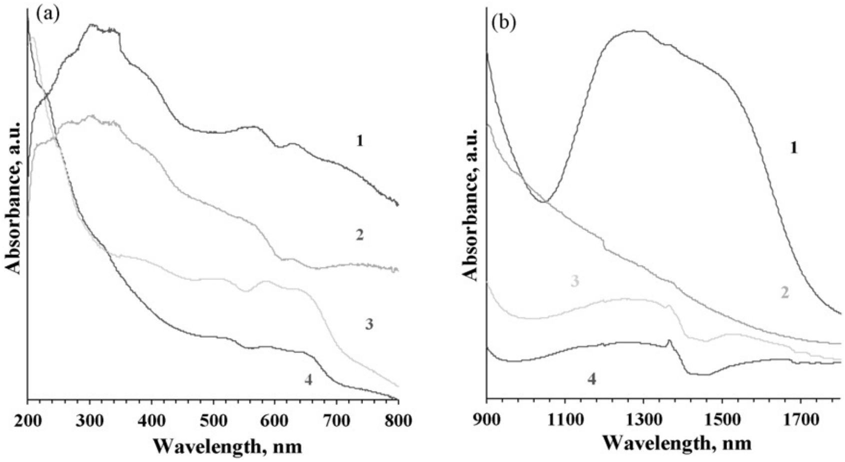

Fig. 2. UV–vis (a) and NIR (b). DR spectra for bulk and supported samples: (1) Co_3O_4, (2) $LaCoO_3$, (3) $LaCoO_x$/MCM-41 and (4) $LaCoO_x/SiO_2$.

supported cobaltate, it may be possible to conclude that all cobalt atoms in $LaCoO_x$/MCM-41 sample are involved into formation of lanthanum cobaltate species. Significantly, the amount of Co(II) calculated per unit mass of Co atoms too much higher for supported $LaCoO_x$/MCM-41 that for the bulk perovskite material. This can be due either to serious structural defects in cobaltate particles resided in the mesopores or to the formation of mixed oxide the nature of which is quite different from $LaCoO_3$. The former mixed oxide contains a part of Co atoms in lower oxidation state (Co(II)) than that in perovskite (Co(III)). EPR spectrum of $LaCoO_x/SiO_2$ sample represents a faint line with $\bar{g} \sim 4.3$ that can be assigned to the isolated Co(II) ions which has also the octahedral coordination to oxygen [7,8]. EPR study shows that in two supported samples Co(II) ions locate in octahedral environments but with different forth and symmetry of local of crystalline fields. Both types of Co(II) site in supported samples are different from Co sites of bulk $LaCoO_3$ and Co_3O_4.

Diffuse reflectance spectra presented in Fig. 2a and b exhibit the bands that can be assigned to cobalt ions located in different environment. As to Co(II) ions in tetrahedral ligand field, the multiplet transition $^4A_2(F) \rightarrow {}^4T_1(P)$ gives rise to a triplet band at 540, 590 and 640 nm. Other transitions like $^4A_2(F) \rightarrow {}^4T_2(F)$ and $^4A_2(F) \rightarrow {}^4T_1(F)$ can be found in near infrared region (NIR) at 1400 and 1600 nm [9,10]. The absorbance spectra for Co(III) ions in octahedral coordination consists of the bands at 340 and 710 nm. These bands correspond to the transitions $^1A_1 \rightarrow {}^1T_2$ and $^1A_1 \rightarrow {}^1T_1$, respectively [9,10]. The Co(II) ions in octahedral coordination can be also presented as defect centers in perovskite structure regarding our EPR data above. According to [9] there exist the following transitions: $^4T_1(F) \rightarrow {}^4T_2(F)$, $^4T_1(F) \rightarrow {}^4A_1(F)$ and $^4T_1(F) \rightarrow {}^4T_1(P)$. The band at 1350 nm in NIR is responsible for the first transition, while other two transitions appear as 570 and 490-nm bands in visible region. The bands below 330 nm are typically assigned to the charge transfer from oxygen to metal in oxide structure [11].

The spectra of supported samples show the bands at 530, 580, 645 nm and very broad bands at ~740 and ~1270 nm (Fig. 2a). From the comparison with the spectra for the bulk perovskite, we could suggest that both supported samples contain Co(II) ions in octahedral environment. At the same time, the small shift of all bands may be interpreted as indicating to some tetragonal distortion of octahedrons in nanosized oxide particles.

Catalytic tests in methanol conversion (Table 2) showed that both the supported samples and mechanical $LaCoO_3$ + MCM-41 mixture are active in the oxidation only (partial and total oxidation), the dehydration does not occur over these catalysts. However, the $LaCoO_x$/MCM-41 exhibits much higher activity in comparison with $LaCoO_x/SiO_2$ (and $LaCoO_3$ + MCM-41) sample. This high activity can be explained not only by the highly dispersion of cobaltate phase inside the pores of MCM-41 but also by the low oxidation state of Co atoms. Moreover, $LaCoO_x$/MCM-41 sample is a powerful catalyst for formaldehyde (CH_2O) production at about 150 °C but also for total oxidation of Volatile Organic Compounds (VOCs) to CO_2 (CO not detectable) after only 200 °C.

A DRIFT "operando" approach (Fig. 3) reveals that the MeOH adsorption on MCM-41 matrix at 50 °C and on both supported samples resulted in the non-dissociative forms of adsorbed alcohol and the formation of methoxy groups. These groups are characterized by the broad band of υOH (3100–

Table 2
Catalytic properties of the samples for methanol oxidation

Catalysts	°C	MeOH conversion (%)	Yield (%)	
			CH_2O	CO_2
$LaCoO_3$ + MCM-41	100	0	0	0
	150	0.5	0.5	0
	175	1.3	0.6	0.7
	200	2.0	0.5	1.5
$LaCoO_x/SiO_2$	100	0	0	0
	150	1.5	0.5	1
	175	2.6	0.7	1.9
	200	3.8	0.9	2.9
$LaCoO_x$/MCM-41	100	2	2	0
	150	37.4	10.4	27.0
	175	67.6	7.2	60.4
	200	97.7	4.1	93.6

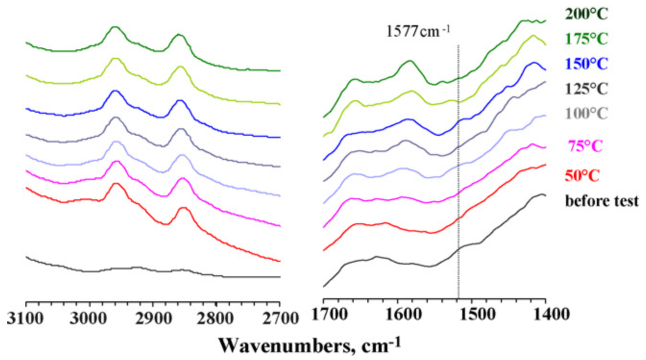

Fig. 3. DRIFT operando catalytic oxidation of methanol on $LaCoO_x$/MCM-41 sample.

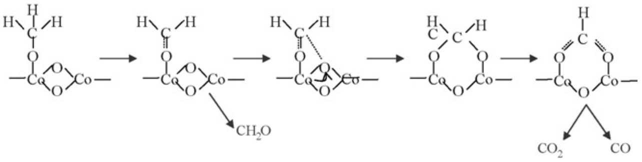

Fig. 4. Proposed mechanism for the both oxidation reactions.

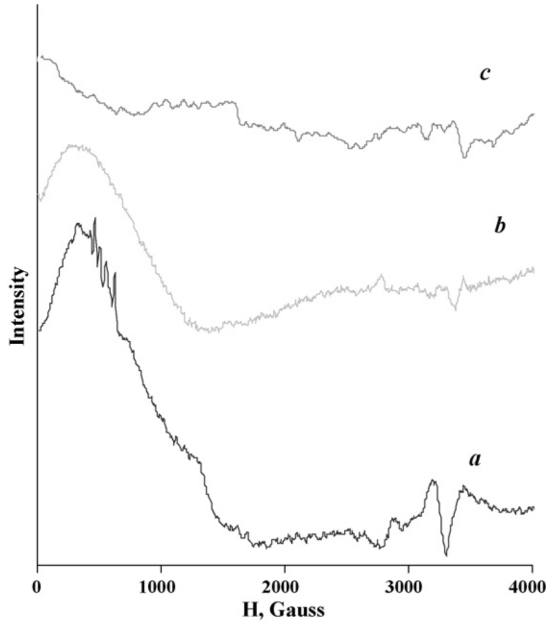

Fig. 5. EPR spectra at $T = 293$ K of $LaCoO_x$/MCM-41 sample before and after catalytic test: (a) before test, (b) after test, (c) the same at $T = 77$ K after test.

3600 cm^{-1}), υ_{sym} and υ_{asym} CH_3 modes (2850 and 2958 cm^{-1}) [12]. Above 75 °C, the formate complex (asymmetric COO stretching at 1577 cm^{-1}) and molecularly chemisorbed water (band at 1660 cm^{-1}) present on $LaCoO_x$/MCM-41 sample but not on $LaCoO_3$ + MCM-41 and $LaCoO_x/SiO_2$. This finding can be explained by rather small surface of cobaltate particles in the case of last two samples and as a consequence of a smaller concentration of absorbed formate species. However, bands of adsorbed formaldehyde as well as adsorbed CO_2 (or carbonate species) were not detected in our spectra.

The mechanism for the both oxidation reactions can be then proposed in Fig. 4.

The EPR spectra of $LaCoO_x$/MCM-41 before and after catalytic tests (Fig. 5) showed that the concentration of octahedrally coordinated Co(II) ions is significantly decreased and a new signal of Co(II) ions (detected only at 77 K) appeared. This signal can be attributed to Co(II) ions coordinated with methanol or other intermediate products of reaction because it could not be seen in the spectrum of the fresh sample. No EPR signals were detected for $LaCoO_x/SiO_2$ after testing in catalysis. This can be due to the changes in Co atoms environments because of coordination with reaction products that makes these atoms EPR silent. It should be noted that after calcination at 400 °C, all spectra became the same as before catalytic test.

To conclude, the conventional citrate method adapted to immobilize the lanthanum cobaltate species within the mesoporous MCM-41 material affords the highly disordered nanosized particles located inside the mesopores of molecular sieve. The use of spectroscopic techniques for the study of methanol oxidation showed that the MeOH oxidation proceeds via the formation of surface formate species and a reaction mechanism is proposed.

Acknowledgements

This work has been supported by the Russian Foundation for Basic Research (grant No. 05-03-32045), the Program for Supporting the Principal Science Schools of RF (RI-112/001/052) and the University of Littoral – Côte d'Opale. E.V. Makshina acknowledges a HALDOR TOPSOE A/S fellowship for PhD students.

References

[1] L.G. Tejuca, J.L.G. Fierro, J.M.D. Tascon, Adv. Catal. 36 (1989) 237.
[2] E.V. Makshina, S.V. Sirotin, M.W.E. Van den Berg, K.V. Klementiev, V.V. Yushchenko, G.N. Mazo, W. Grünert, B.V. Romanovsky, Appl. Catal. A: Gen. 312 (2006) 56.
[3] S.V. Nguyen, V. Szabo, D. Trong On, S. Kaliaguine, Micropor. Mesopor. Mater. 54 (2002) 51.
[4] M.S.G. Baythoun, F.R. Sale, J. Mater. Sci. 17 (1982) 2757.
[5] H. Gies, S. Grabowski, M. Bandyopadhyay, W. Grünert, O.P. Tkachenko, K.V. Klementiev, A. Birkner, Micropor. Mesopor. Mater. 60 (2003) 31.
[6] M.A. Heilbron, J.C. Vickerman, J. Catal. 33 (1974) 434.
[7] A. Abragam, B. Bleany, Electron Paramagnetic Resonance of Transition Ions, vol. 1, Claredon Press, Oxford, 1970.
[8] A. Carrington, A.D. MacLachlan, Introduction to Magnetic Resonance with Applications to the Chemistry and Chemical Physics, Harper & Row Publishers, New York, 1967.
[9] A.B.P. Lever, Inorganic Electronic Spectroscopy in Studies in Physical and Theoretical Chemistry, vol. 33, Elsevier, Amsterdam, 1984 (Chapter 6).
[10] C.J. Ballhausen, Introduction to Ligand Field Theory, McGraw-Hill, New York, 1962.
[11] M. Karthik, A.K. Tripathi, N.M. Gupta, A. Vinu, M. Hartmann, M. Palanichamy, V. Murugesan, Appl. Catal. A. 268 (2004) 139.
[12] G. Busca, Catal. Today 27 (1996) 457.